SEISMIC ATTENUATION CHARACTERIZATION USING TRACKED VEHICLES

James F. Scholl, Loren P. Clare and Jonathan R. Agre
Rockwell Science Center
Thousand Oaks, CA 91360

ABSTRACT

Target classification is one of the most important issues in battlefield situational awareness. As seismic signals are an effective means of obtaining such information, any knowledge of the subsurface environment in which the target signal propagates is very important in either developing or fine-tuning classification algorithms. Seismic signal attenuation is an essential subsurface environmental characteristic and is known to be frequency dependent. We first describe a simple method for computing seismic attenuation using a single seismic measuring device and a large tracked vehicle with known tread spacing characteristics. Following this, we extend the method to an array of randomly placed sensor nodes. We first illustrate this method for a single node by means of tracking the size of certain spectral features in measured seismic data. For example, the seismic signature of an M60 tank has a distinct peak at a specific frequency depending on its speed. Given the distance to CPA and the vehicle speed, a portion of the signal corresponding to a given distance from vehicle to sensor can be examined and the power spectral density of that peak measured corresponding to that distance. From this type of data, attenuation profiles can be measured as a function of distance for various frequencies. Seismic attenuation parameters can be computed from the profiles using suitable regression techniques. Data collected for sensor arrays will be analyzed and compared with the single sensor results to assess local ground effects. Also, we will compare the ability of an array of sensors to characterize the ground using an impulsive source with the moving vehicle source. This then characterizes the seismic medium and can assist in classification of general targets.

1.0 INTRODUCTION

This paper discusses a method for computing seismic attenuation using a single sensor and a single vehicle, usually tracked. Such physical behavior is important because many classification schemes are either frequency based, or are time-frequency based decompositions of the signal collected at the sensor. Misclassification of vehicles can happen at large distances away from the closest point of approach (CPA). The reason for this is due to the vehicle traveling at different speeds; here for tracked vehicles, tread slap (to be discussed more fully below) changes the peak frequency of the seismic power spectra. Other mechanical attributes of a motorized vehicle that are speed dependent also contribute to changing a vehicle's power spectra; not taking these into account can also result in misclassification.

However if we concentrate on the case where a tracked or wheeled vehicle moves at a constant speed towards, past and away from CPA, then we still observe classification that is a consistent function of distance as well as frequency [1, 2]. The origin of this behavior is seismic attenuation. It is well known that the ground acts as a lowpass filter. High frequency seismic energy from a tracked or wheeled vehicle will not travel as far as energy with low frequency content. The attenuation will be different for various soil, rock, and surface types.
[1]

Knowledge of seismic attenuation is useful in that this gives some idea of the range of a vehicle, especially a tracked one as a function of speed. As spectral information from fast vehicles is here peaked at higher frequencies than with slower vehicles, seismic attenuation will reduce the energy from these faster vehicles at a farther distance.

The views and conclusions contained in this document are those of the authors and should not be interpreted as presenting the official policies, either expressed or implied of the Army Research Laboratory or the U. S. Government.

Report Documentation Page

Report Date	Report Type	Dates Covered (from... to)
00 Aug 1999	N/A	-

Title and Subtitle Seismic Attenuation Characterization Using Tracked Vehicles	**Contract Number**
	Grant Number
	Program Element Number
Author(s)	**Project Number**
	Task Number
	Work Unit Number
Performing Organization Name(s) and Address(es) Rockwell Science Center Thousand Oaks, CA 91360	**Performing Organization Report Number**
Sponsoring/Monitoring Agency Name(s) and Address(es) Department of the Army, CECOM RDEC Night Vision & Electronic Sensors Directorate AMSEL-RD-NV-D 10221 Burbeck Road Ft. Belvoir, VA 22060-5806	**Sponsor/Monitor's Acronym(s)**
	Sponsor/Monitor's Report Number(s)

Distribution/Availability Statement
Approved for public release, distribution unlimited

Supplementary Notes
See also ADM201471, Papers from the Meeting of the MSS Specialty Group on Battlefield Acoustic and Seismic Sensing, Magnetic and Electric Field Sensors (2001) Held in Applied Physics Lab, Johns Hopkins Univ, Laurel, MD. on 24-26 Oct. 2001. Volume 2 (Also includes 1999 and 2000 Meetings)

Abstract

Subject Terms

Report Classification unclassified	**Classification of this page** unclassified
Classification of Abstract unclassified	**Limitation of Abstract** UU

Number of Pages
10

Furthermore, knowing the seismic attenuation at an area as well as the frequency or time-frequency characteristics of different vehicles at various speeds also provides some measure of classification reliability. This is especially useful for networks of seismic sensors.

We propose a method for seismic attenuation estimation based on the fact that a tracked vehicle at different constant speeds will exhibit a shifting of its dominant spectral energy peak due to velocity based tread-slapping. The range of this shift is from 20 Hz to 50 Hz. We also see this in a data collection exercise where instead of a tank, we fit tire chains on a heavy wheeled vehicle (an SUV) and observed this effect in some degree. Since we know the wheel/tread geometry, in addition to the speed of the vehicle we can measure the spectral peak power as a function of distance. Compiling such peak tracking data at various speeds we can estimate by fitting the data to a simple seismic attenuation model. We also computed seismic attenuation using a network of sensors simultaneously recording an impulse signal and doing spectral peak tracking as a function of sensor-impulse distance.

This paper is organized as follows. Section 2 will discuss seismic attenuation and the standard model we adopted in our work. Section 3 will discuss the two different methods used to compute seismic attenuation as well as the seismic sensors we used for our calculations. In section 4 we will present results from field measurements and how the two methods compare with each other. Section 5 discusses ways to use seismic attenuation information as a measure of classifier reliability as well as for simulation. Section 6 is the conclusion.

2.0 SEISMIC ATTENUATION

2.1 Seismic Attenuation and Target Classification

Related to this, information from models of how tracked or wheeled vehicles behave as they couple to the ground typically get expressed as power spectra. An excellent example of this is given by Coney and Galaitsis [3]. These reasonable models and simulations justify the frequency or time-frequency based classification algorithms. Naturally, information from such models will be hard to test as well as hard to exploit in the field when there is significant attenuation in seismic energy in both distance and frequency.

Many seismic classification algorithms depend on decompositions in frequency or in time and frequency. As long as seismic energy gives an overall power spectral signature in the low frequency end of the spectra, then classification is reliable on the order of hundreds of feet. As was shown by Scholl et al [1-2], seismic attenuation was responsible for misclassification for some vehicles at large distances due to attenuation of key higher frequency features in the range of 45-75 Hz that were characteristic of certain vehicles but not others. The type of seismic waves we deal with in this paper are Rayleigh waves which travel along the top layers of the ground and with frequencies lower than 80-100 Hz.

2.2 Description of Seismic Attenuation Model

We use as the model [4] of attenuation for spectral density S(x,f)

$$S(x,f) = S(0,0)\, e^{-\kappa x f} \qquad (1)$$

Where S(x,f) is the spectral density of a seismic signal from a target at distance x to CPA as a function of frequency f. S(0,0) is the spectral density of the target at DC power when it is at CPA; usually this is not known. What we are estimating is the seismic attenuation parameter κ.

In addition to their being attenuated in amplitude, seismic signals in the form of impulses are well known theoretically to get broadened as they travel [5]. We observe this behavior to some extent in field measurements. The behaviors of seismic attenuation and pulse broadening are also seen quite clearly in field data. For example Figure 1 illustrates seismic attenuation for an impulse signal as seen by sensors at 5 feet, 41 feet, 61 feet and 100 feet from the source; here we keep the vertical scale the same so that the diminution of amplitude is very evident. On the other hand in Figure 2 we took the identical signals and plotted them with the same scale in time, but with

the vertical scale in step with the amplitude of the pulse; we clearly see the broadening of the pulse as it moved through the medium. The impulse source was a sledgehammer hitting a metal plate on the ground.

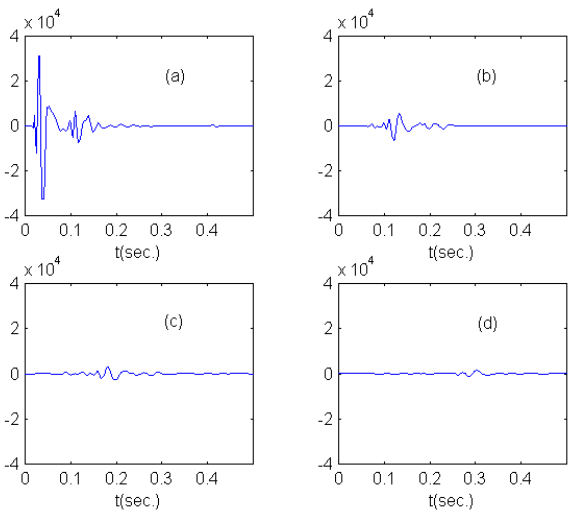

Figure 1: Seismic attenuation of an impulse signal created with a sledgehammer hitting the ground as mentioned above. The vertical scales are the same to emphasize the attenuation. The signal has been recorded with sensors (a) 5 feet, (b) 41 feet, (c) 61 feet and (d) 100 feet from the source.

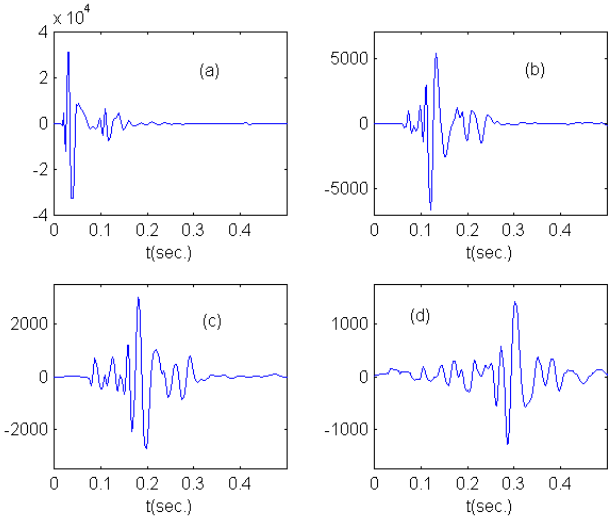

Figure 2: Broadening of an impulse signal created with a sledgehammer hitting the ground as mentioned above. The vertical scales are different to emphasize the pulse broadening. The signal has been recorded with sensors (a) 5 feet, (b) 41 feet, (c) 61 feet and (d) 100 feet from the source.

However, the pulse broadening from impulse signals does not significantly affect our calculations, the details of which are discussed in section 3. This is because the distance scale of our calculations is on the order of tens up to a few hundreds of feet (~3 to 100 m) and the broadening is not that severe. This sort of behavior is also not prominent for more complicated seismic signals, mainly those that come from wheeled and tracked vehicles over the same distances. However, in the case where seismic sensors are spread over hundreds of meters or feet, then

broadening may have to be taken into account. In this paper the distance scales are such that signal broadening can be ignored.

We will also see that for relatively small scales many geophysical and geological parameters such as attenuation vary considerably. Larger scale field measurements will most likely result in more relatively uniform estimates of physical parameters. In practice an average value of attenuation in a small area from a group of sensors will be adequate enough for use in target classification, with the proviso that the variation is not severe and that there is a particularly large or small value at a particular sensor location. Such outlier estimates of the attenuation coefficient κ can result from either faulty sensors or some aspect of the subsurface geology localized at that location.

3.0 SEISMIC ATTENUATION MEASUREMENTS AND CALCULATIONS

3.1 Wireless Seismic Sensors

An important class of emerging networked embedded systems for many DoD applications is distributed microsensor networks. In the not too distant future, a single ultra low power CMOS chip that integrates radio communication, digital computing, and MEMS sensing components on a single die will be realized. A large number of such wireless microsensors may be airdropped into battlefields to form highly redundant self-organizing and self-configuring ad hoc sensor networks, or may be used to create easily and rapidly deployable sensor networks for other military and civilian applications such as premise security and surveillance and equipment monitoring.

Rockwell Science Center has developed a wireless microsensor node based on an open and modular design using COTS technology under an existing DARPA program called AWAIRS (with UCLA) [6]. Currently, two hundred units are being produced. These nodes combine multi-modal sensing capabilities (seismic, magnetic, pressure, temperature, acceleration, high-speed vibration) with a short-range radio and a low-power embedded StrongARM RISC processor in a small package powered by 9V batteries. Figure 3 shows the Rockwell wireless microsensor node and its cross-section.

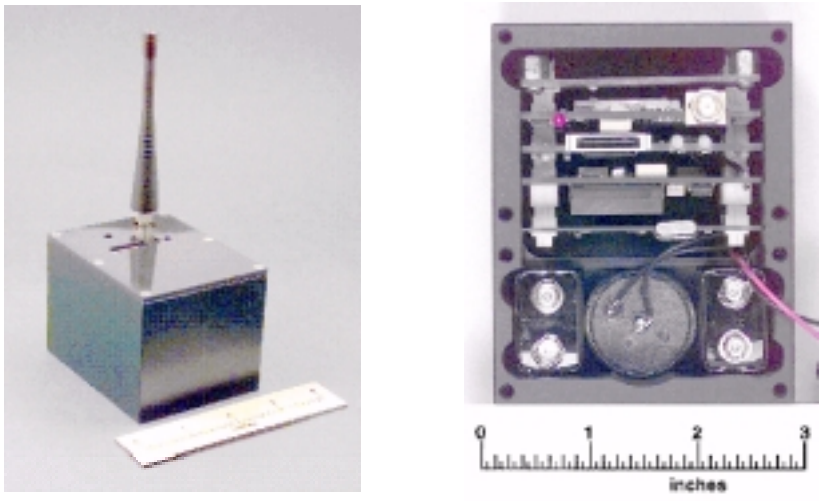

Figure 3: Rockwell's wireless sensor node and cross-section

3.2 Impulse Based Attenuation Determination

Computing the seismic attenuation constant $\kappa(x,f)$ where x is the distance (feet or meters) and f the frequency in Hz is generally straightforward from field data. We assume that the sensor locations are known as well as the position of where a test impulse signal is generated. Signals like those presented in Figures 1 and 2 will then be recorded; note that the ground's response to the impulse (in this example a hard sledgehammer blow) is not exactly impulsive. In fact the ground and the sensor will tend to "ring," and the spectrum will show a variety of

features (Figure 3). We then track each prominent feature in the frequency domain and then measure the power of that feature as a function of distance from the source.

If we have N frequency features at frequencies f_n, n=1,N measured at M sensors each at distance x_m, m=1,M then we get an M x N table of power spectra features S_{mn} of the form $\{x_m, f_n, S_{mn}\}$. We then take the data and fit that directly to a model described by equation (1) using standard regression routines that can be found in various statistical, mathematical or data analysis / plotting software platforms. We can also estimate S(0,0), but this number is not as important as that of $\kappa(x,f)$.

3.3 Vehicle Based Attenuation Determination

If we use tracked vehicles to measure attenuation, then we do not have information to compute S(0,0); this is mainly due to two reasons. First, the seismic energy from tracked vehicles generally is not concentrated at zero frequency, but at various frequencies at various speeds and mechanical conditions. Secondly, it is impracticable to position a sensor for a CPA at zero distance. However, tracked vehicles have a characteristic track pitch ρ as illustrated in Figure 4.

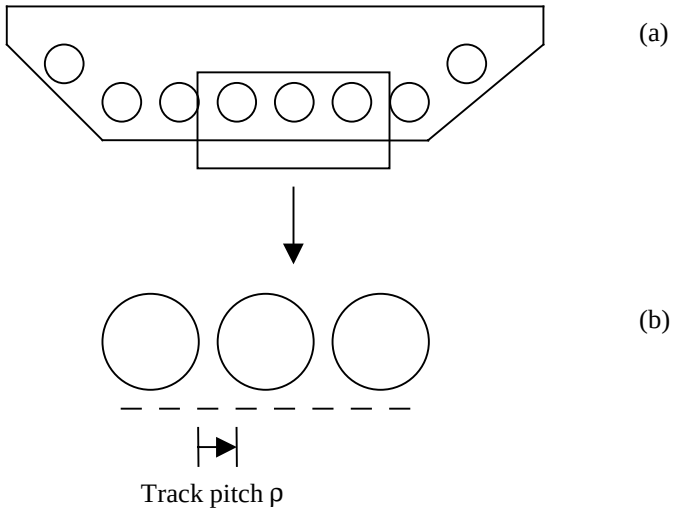

Figure 4: (a) Schematic of tracked vehicle. (b) Schematic of track pitch.

If we know the track pitch ρ and the speed of the vehicle v we obtain the tread slap frequency f_v for that particular vehicle at that speed from the relation $f_v = \rho/v$. The peak in the seismic power spectra corresponding to the tread slap will move toward higher frequencies as the vehicle moves at higher speeds. The track pitch for various tracked vehicles we examined varies from 15 to 20 cm.

This gives us an alternate means to compute seismic attenuation by tracking these tread slap peaks. If we know the speed v that is assumed constant, the CPA distance and the vehicle's geometry on a course (usually a straight line), then we have enough information to compute $\kappa(x,f)$.

The overview of our algorithm is as follows. For each signal corresponding to a fixed constant velocity v, and hence f_v, we fit an attenuation profile of the form $e^{-\alpha v(f)x}$ where $a_v(f)$ is the attenuation function. We measure the peak power corresponding to each separate track frequency f_v. Once we have obtained enough values of $\alpha_v(f)$ corresponding to various speeds and f_v values, we then fit a model of the form $\alpha_v(f) = \kappa f$, finally getting our estimate of the attenuation constant. The details of this algorithm are summarized below.

Algorithm 1:
Seismic Attenuation Estimates from Tracked Vehicle Tread Slaps

1) Record seismic sensor data from vehicles at N different known constant speeds v(n), n=1,N. Obtain time of CPA and distance to CPA for each signal.
2) For each signal n, n=1,N:
    3) Extract M subsets corresponding to the vehicle being at distances x_m, m=1,M from the sensors. This is easily done since we know the vehicle's speed and distance to CPA.
    4) Compute power spectra corresponding to each x_m. Measure power at the peak with frequency given by the equation $f_{v(n)} = \rho/v(n)$, or if ρ not known for the vehicle, at the dominant peak frequency.
    5) Fit the attenuation profile to the model $e^{-\alpha v(n)(f)x}$.
6) From the n values of $a_{v(n)}(f_{v(n)})$, compute k using the model $\kappa = \alpha_v(f)f$.

Although κ is a fitted function of frequency, we implicitly say $\kappa = \kappa(x,f)$ since the $\alpha_v(f)$ were fitted attenuation profiles from spectral peak powers at various distances x from the sensor.

4.0 RESULTS

4.1 Data Collection Exercise

We obtained data for attenuation calculations at two sites. All the seismic data collected at both sites was sampled at 400 Hz.

The first site was at the Aberdeen Proving Grounds in Maryland in December of 1998. A single seismic sensor of the type described in Section 3.1 shown in Figure 3 was used. A portion of the data collected was a series of runs from an M60 tracked vehicle traveling at constant speeds of 5, 10, 15 and 20 miles per hour with a CPA of 29 feet. We used this data to help us develop the vehicle based seismic attenuation algorithm given above. Here, only one value of κ was estimated. The best fit of κ from the data was about 2.0×10^{-4} seconds/feet.

The second data collection exercise was held near Van Nuys, California at the Sepulveda Dam basin, in June of 1999. Here the soil type was recently compacted and graded dry clay. We collected seismic data from nine (9) sensors. Figure 5 shows the sensor locations at the data collection site. The position of node 115 was designated as the origin. We measured attenuation from impulses (Figures 1 and 2) at two places at the site, and recorded vehicle data. The CPA from the vehicle to all the sensors was seven (7) feet. Each line of sensors was 14 feet apart, and the sensors on one line were 20 feet apart. The sensors on the other line were 30 feet apart.

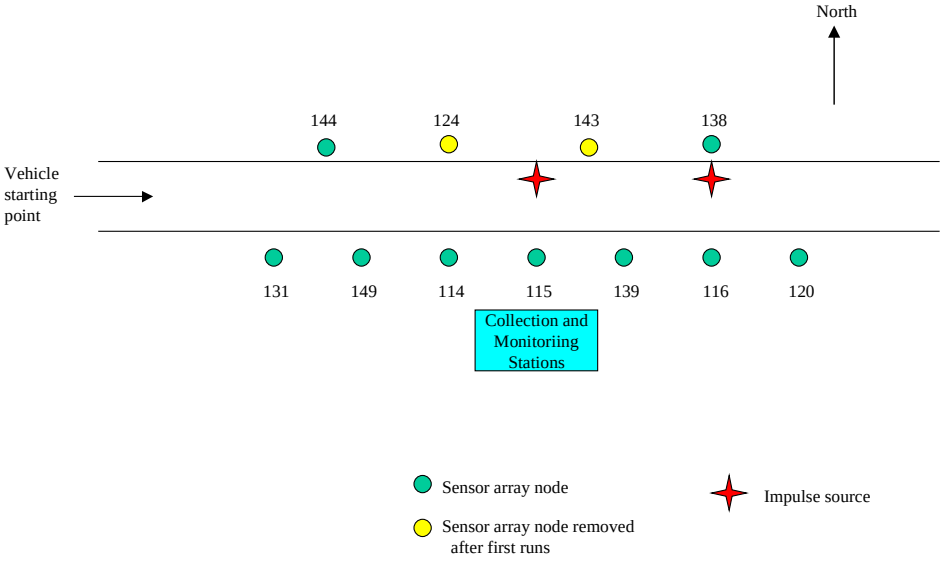

Figure 5: The schematic of the data collection site near Van Nuys, California at the Sepulveda Dam basin. Nodes 124 and 143 were not used to take data used for seismic attenuation determinations.

The vehicle used for the runs was a sport utility vehicle (SUV) with tire chains with runs by the nodes of 5, 10, 15 and 20 miles per hour. The power spectra from the seismic data for all runs had a dominant peak that shifted towards the higher frequency as the vehicle went faster, just like that of a tracked vehicle.

We then estimated the seismic attenuation coefficient κ from impulses as well as with the SUV at each node using the algorithms discussed in sections 3.2 and 3.3. We also computed the mean squared error (MSE) for each estimate. All data analysis and regression computations were done using Matlab v.5.3 [7] and Mathematica v.3.0 [8]. The results of the attenuation calculations from both Aberdeen Proving Grounds and Sepulveda are presented in Table 1.

Table 1. Attenuation coefficient calculation results from Sepulveda

Type of Calculation	Sepulveda coordinates (feet)	κ in seconds/feet	MSE (normed,unitless)
Impulse mid-array	(0,9)	0.00137	0.0202
Impulse end of array	(40,9)	0.00101	0.0407
Vehicle @ node 131	(-60,0)	0.00152	0.0499
Vehicle @ node 144	(-50,14)	0.00161	0.0576
Vehicle @ node 149	(-40,0)	0.00134	0.0759
Vehicle @ node 114	(-20,0)	0.00170	0.0523
Vehicle @ node 115	(0,0)	0.00158	0.0567
Vehicle @ node 139	(20,0)	0.00186	0.0469
Vehicle @ node 138	(40,14)	0.00214	0.0441
Vehicle @ node 116	(40,0)	0.00192	0.0639
Vehicle @ node 120	(60,0)	0.00170	0.0789

Our results indicate that over the small area represented in Figure 4 the value of κ has some variation. There are probably two values of κ that may be outliers; the impulsive source at the end of the array with κ=0.00101 seconds/feet and the vehicle based attenuation measurement at node #138 with κ=0.00214 seconds/feet. However, the MSE values are all relatively similar to each other. This likely means that both methods of computing seismic attenuation generally are equally reliable.

Finally, the seismic attenuation profile corresponding to κ for the vehicle derived attenuation at node #116 (0.00192 seconds/feet and κ computed from the impulse at mid array (0.00137 seconds/ft) are shown in figures 6a and 6b respectively.

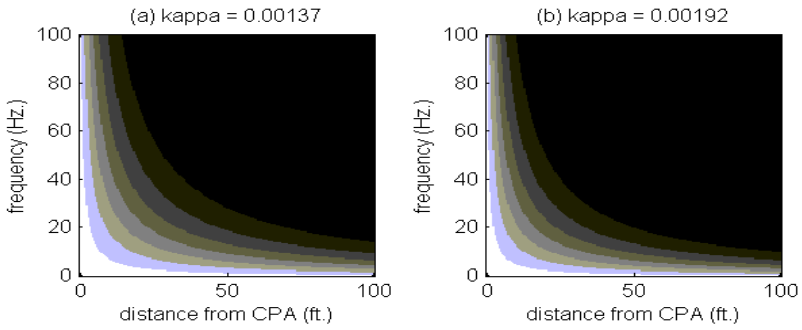

Figure 6: Seismic attenuation profiles from the data collection exercise near Van Nuys, CA, illustrating the range of values of κ computed from field data. (a) Attenuation profile from κ computed from impulsive signal generated near middle of data collection area, (b) Attenuation profile from κ computed from vehicle data passing node #116.

5.0 PROPOSED IMPROVEMENTS IN TARGET CLASSIFICATION USING ATTENUATION ESTIMATES

5.1 Seismic Target Classification Confidence Levels

We can use estimates of seismic attenuation as a function of distance and frequency as a means to compute reasonable confidence levels of a seismic sensor's classification results. We assume that we have seismic target classification algorithms that involve matching of bin / subband data in the frequency domain of which [1] is an example. That is, for a given tracked or wheeled vehicle at a given speed we have a reference 'vector' of length N (i.e., number of bins, subbands). These reference vectors are usually computed from signals obtained when a target is at CPA. Let d_{CPA} be the CPA distance of the vehicle to a test sensor when the signals used for reference vector generation are made. A transform (Fourier or wavelet packet) is made of that data, and the PSD coefficients in each of N frequency bins or squared value of the wavelet packet coefficients in each of the N subbands are averaged. Hence for the jth vehicle in our collection of vehicle data we have a reference vector $\mathbf{V}_j = \{v_{j1}, v_{j2}, \ldots, v_{jN}\}$, each v_{ji} represents the average in the ith PSD frequency bin or ith wavelet or wavelet packet subband. Usually, the coefficients $\mathbf{V}_j$ are normalized such that the scalar product $\mathbf{V}_j \bullet \mathbf{V}_j \equiv 1$. As each bin or subband has an average signal frequency, these bins or subbands each has an f_i value.

Since each vehicle with a given speed has different signatures over the frequency domain, it is then safe to assume that seismic attenuation will essentially give each reference vector a classification range. Reiterating what was said above, vehicles with identifying features in the lower frequencies will be classified more successfully farther away than vehicles with a great deal of higher frequency features. We can quantify this. We propose the attenuation-classification confidence measure $C^j(x)$ for vehicle j at distance $x = |d - d_{CPA}|$ where d is the distance of the vehicle to the sensor and d_{CPA} the CPA distance defined above. Then:

$$C_j(x) = \frac{\sum_{i=1}^{N} v_{ji} e^{-\kappa(x,f) x f_i}}{\sum_{i=1}^{N} v_{ji}} \quad . \qquad (2)$$

This measure is valid for the situation where we have an array of sensors in the field and that some sort of target location algorithm used. Then $C_j(x)$ can be measured at sensors which pick up the seismic signal from the putative target j. A threshold C_j^{thresh} for identification of target j is implied; if a sensor initially classifies a seismic signal signature as being object j, then if $C_j(x) < C_j^{thresh}$ the classification would still be considered uncertain.

5.2 Simulation of Seismic Target Signatures

With seismic attenuation estimated as a function of both distance and frequency we can simulate what the seismic signal signature is going to look like for a given vehicle at a given speed at an arbitrary distance. This is the 'inverse' of the principle behind vehicle based attenuation. If we know the signature of a tracked (or wheeled) vehicle in frequency either by direct measurement at a close CPA distance or by simulation as in [3], then in principle we know how that signature changes as a function of time and distance.

In tracked vehicles, especially once the speed is known, then a time-frequency plot that factors in attenuation as well as site geometry can be simulated. This would give us a computational test-bed to improve classification algorithms as the predicted frequency or time-frequency information can be compared to measurements in the field.

For example, Figures 7a-b illustrate such a simulation from the data collection exercise at Aberdeen Proving Grounds last December. An actual spectrogram of the seismic data of a light tracked vehicle is given as figure 7a. Figure7b is a simulated spectrogram given the PSD of the vehicle at CPA and a $\kappa = 0.0003$ seconds/feet; it is not a perfect simulation, because of other factors such as noise and possibly seismic / above ground acoustic coupling. What is important is that such simulation is possible.

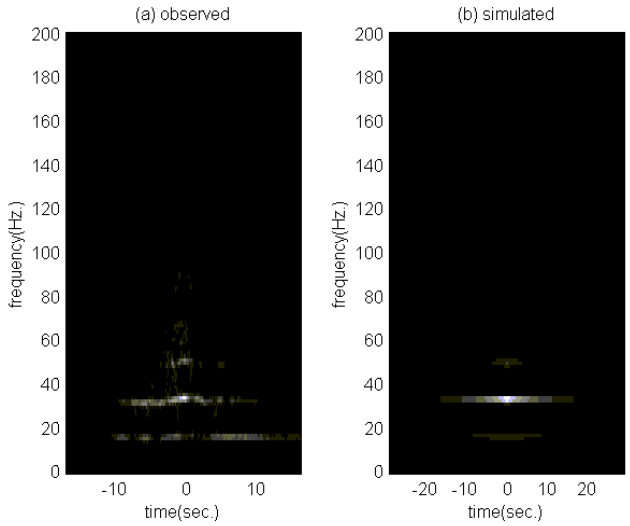

Figure 7: The actual and simulated spectrograms of a light tracked vehicle (MLRS) traveling at 20 mph. The left-hand figure (a) was obtained from field data. The right-hand (b) spectrogram was simulated from the PSD coefficients of the data and κ of 0.0003 seconds/feet. The sampling rate was 400Hz and time 0 corresponds to CPA of the vehicle to the sensor.

6.0 CONCLUSION

We have shown that it is feasible to calculate seismic attenuation characteristics at a given spatial location using a single sensor and a tracked vehicle passing by it at various constant speeds and known CPA distance. This is done by tracking the magnitude of the dominant power spectra peaks that change in frequency as the vehicle

changes speed. Since the CPA distance and vehicle distance are known, we can select a piece of the time series and compute the PSD corresponding to arbitrary distances from the sensor.

We have also shown that the MSE in determining the seismic power attenuation coefficient κ from vehicles and a single sensor as compared to the MSE in determining κ from an impulse signal with multiple sensors are comparable to each other. Nevertheless, there is room for improvement as indicated by the MSE. This situation will be improved once more sensors are available in the field. Hence one has two choices in computing seismic attenuation depending on field conditions and situations; there may be cases where one method for computing the seismic attenuation is better than the other one. However, arrays of sensors will mitigate the effects of individual sensor problems or local geological effects.

We have also suggested how computation of κ can be used to calibrate seismic classification algorithms and can be used for data simulation.

Finally, we have also shown that there is a fair amount of short-range variability in seismic attenuation over a scale of tens of feet. How important this variability is in classification is yet to be determined.

7.0 SUPPORT

This work was supported in part by the ARL Advanced Sensors Consortium, Contract No. DAAL01-96-2-0001.

8.0 REFERENCES

[1] J. F. Scholl, J. R. Agre, and L. P. Clare, "Wavelet Packet Based Target Classification Schemes," *Proceedings, 1998 Meeting of the IRIS Specialty Group on Acoustic and Seismic Sensing*, Laurel, MD, 29 Sept. – 1 October 1998, pp. 79-95.

[2] J. F. Scholl, J. R. Agre, L. P. Clare, and M. C. Gill, "Effects of Seismic Attenuation on Signal Classification," *Proceedings, 3rd Annual Federated Laboratory Symposium on Advanced Sensors*, College Park, MD, 2-4 February 1999, pp. 93-97.

[3] W. B. Coney and A. G. Galaitsis, "Exploratory Predictions of Tracked Vehicle Signatures," *Proceedings, 1998 Meeting of the IRIS Specialty Group on Acoustic and Seismic Sensing*, Laurel, MD, 29 Sept. – 1 October 1998, pp. 97-110.

[4] A. H. Balch and M. W. Lee, "Vertical Seismic Profiles," in *Vertical Seismic Profiling: Technique, Applications and Case Histories*, A. H. Balch and M. W. Lee, editors, (Boston: International Human Resources Development Corporation), pp. 3-67 (1984).

[5] J. E. White, *Seismic Waves: Radiation, Transmission, and Attenuation*, (New York: McGraw-Hill), (1965).

[6] http://www.janet.ucla.edu/lpe.lwim/

[7] The MathWorks Inc., *Using Matlab*, Natick, Mass, (1997).

[8] S. Wolfram, *The Mathematica Book*, Third Edition, Cambridge University Press, (1996).